Fatigue and Ultimate Strengths of Concrete Filled Tubular K-Joints on Truss Girder

Pison UDOMWORARAT*, Chitoshi MIKI**, Atsushi ICHIKAWA**,
Eiichi SASAKI***, Takuya SAKAMOTO****, Kaoru MITSUKI***** and Tetuya HOSAKA******

* M. Eng., Graduate Student, Dept of Civil Eng., Tokyo Institute of Technology, Tokyo 152-8552
** Dr. of Eng., Professor, Dept of Civil Eng., Tokyo Institute of Technology, Tokyo 152-8552
*** M. Eng., Research Associate, Dept of Civil Eng., Tokyo Institute of Technology, Tokyo 152-8552
**** Graduate Student, Dept of Civil Eng., Tokyo Institute of Technology, Tokyo 152-8552
***** Hokuriku Shinkansen Construction Dept., Japan Railway Construction Public Corporation, Nakano
****** Design Technology Dept., Japan Railway Construction Public Corporation, Tokyo

This study focuses on improving the fatigue performance and ultimate strength of welded steel tubular joints. In order to improve the structural performance of the panel point joint of truss, concrete is used to fill the hollow tubes in the region of the joint. The behavior of unfilled and filled joints was examined through analysis and testing. The analytical and experimental results suggest substantial improvement in the fatigue performance as well as the ultimate strength of concrete-filled welded steel tubular joints as compared to unfilled joints.

Key Words: Welded Steel Tubular Joints, Ultimate Strength, Fatigue Strength, Stress Concentration Factor, Concrete Filled Tubular Joints

1. Introduction

Steel tubular members are used in many structural systems for several reasons: very good post-buckling behavior, Omni-directional strength offering design flexibility and greater economy in mass, and favorable aerodynamic and hydrodynamic properties. In addition, structures made of tubular members have a smaller surface area than comparable structures of open sections. The absence of sharp corners, combined with a smaller surface area, results in a better performance of corrosion protection. When used in structures subjected to repetitive or cyclic loads, however, fatigue problems can occur in and near welded tubular joints.

This study focuses on the tubular K joint as used in the design of railway truss girder bridges. The bridge under consideration is a through-truss type with parallel upper and lower chords connected with all-diagonal panel members. A dominant factor affecting fatigue resistance of the tubular truss girder is localized high stress concentrations at the intersections of chord and diagonal panel members. The local high stresses are the result of local bending and membrane stresses in the crown of the chord members between the diagonal members. The stresses in this critical region can vary greatly because of global and local geometric parameters: overall connection configuration, tube diameter, wall thickness, stiffener details, and even weld bead profiles.

The fatigue strength of welded tubular joints is quite sensitive to the local stress concentration. The severity of the local stresses is usually expressed in terms of a stress concentration factor (SCF) normalized against the nominal stress in a given diagonal panel member. Even a modest reduction in SCF can result in substantial gains in fatigue life. It was observed in a previous study that partially filling tubes with grout might lower the SCF in the critical region[1]. The previous study of grout joints mostly focused on pile-to-sleeve connections or some repairing joints in offshore structures where chord could be treated as fixed conditions and only main applied forces were applied on both brace members. Because truss girders of tubular members have been only applied to building and small girders such as water pipeline bridge. In design of truss bridge, the behaviors of filled concrete joints are not so much clear due to the lack of study information.

In this study, we examine the effects of filling the tubes with concrete only in the joint region. In actual bridges, the lengths of tube remote from the joint are to remain hollow. This is done to minimize the increase in dead weight of the members, which are an especially important consideration for most bridge structures. Once cured, the concrete stiffens the joint by reducing the amount of ovalization in the framing members. In this way, the local bending and membrane stresses can be reduced which in turn lowers the SCF values in critical regions. In addition, the concrete increases resistance to local buckling, and offers some composite action thereby affording increases to ultimate strength capacity.

2. Model Bridge

The bridge was preliminary designed as three equal spans continuous truss bridge. Each span has 68 m. in length, 4.7 m. in width and 8 m. in height, respectively. The design was also emphasized on effective dimension and thickness of the members, which could be satisfied loading condition. Symmetrical half-structural model of the designed bridge was developed by using three dimensional frame finite element analysis to examine critical joint that might subject to a very severe fluctuated load condition from passage trains. In this case, the most critical joint was adopted as a representative tubular K joint section in this study. From the analysis, many load case conditions may induce a very high stress concentration at the joint. Therefore, a simplification of the selected critical load case with leading to the set up of testing specimen is in anti force directions of the diagonal members as shown in Fig.2. At last, we could approximately obtain the dimension of 600 mm. diameter chord and 400 mm. diameter diagonal members. Fig.1 shows the bridge dimensions and the location of the critical K joint.

3. Specimens

Two different types of tubular K joint were considered in the tests and analysis activities of this study (see Fig. 3). The two types, which are hollow (type I) and concrete filled (type II) sections, had been tested under constant amplitude loading in fatigue test. Ultimate strength tests were conducted on two specimen types. Three-dimensional nonlinear finite element models were constructed to examine each of the K joint details. Fig.3 shows K joint details of type I and type II. All the K joints are ½-scale model and have ratios of diagonal member diameter to chord diameter $\beta = d/D = 0.68$, chord length to chord diameter $\alpha = 2L/D = 8.73$, chord diameter to chord thickness $\gamma = D/2T = 23.42$ (see Fig.4).

Type I joints consist of 318.5 mm. and 216.3 mm. diameters of chord and diagonal members, respectively. Both of the diagonals had been welded 60 degrees from the horizontal level with the gap between intersection point of the diagonals and the chord at distance of 60 mm. At welded area, 2-3 layers of full penetration weld were filled in cutting V groove along intersection perimeter. Cutting profile at inner crown location was shown in Fig.5.

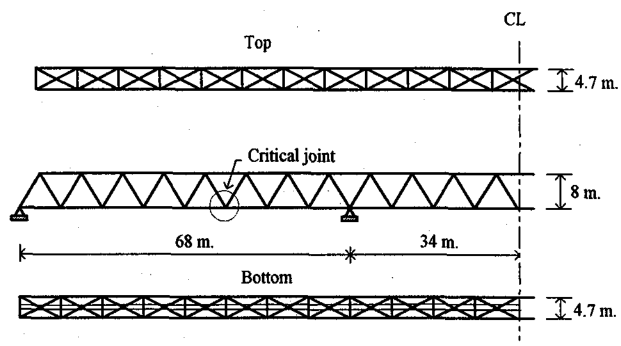

Fig.1 Model bridge dimensions

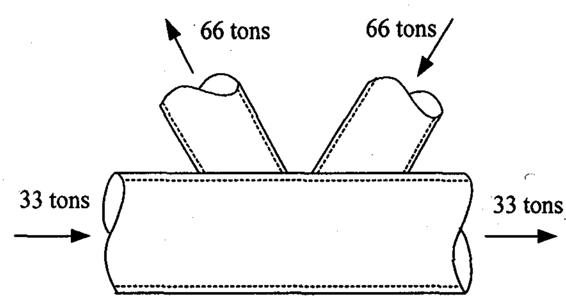

Fig.2 Simplification of applied load

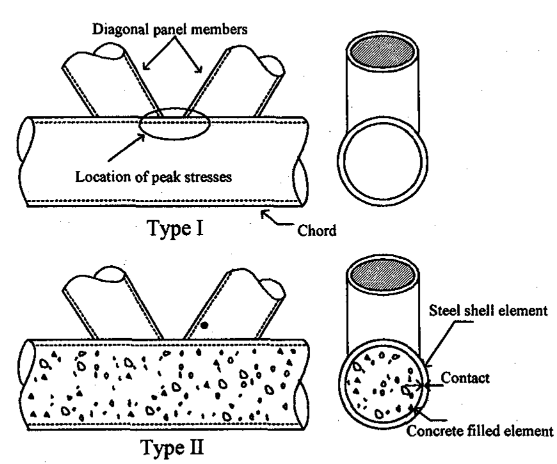

Fig.3 K joint details and the location of peak stresses

Type II is identical to type I joint. However, concrete completely filled inside chord member. The idea is that large deformation of chord wall due to secondary bending deformation can give a very large stress concentration near to the weld toe.

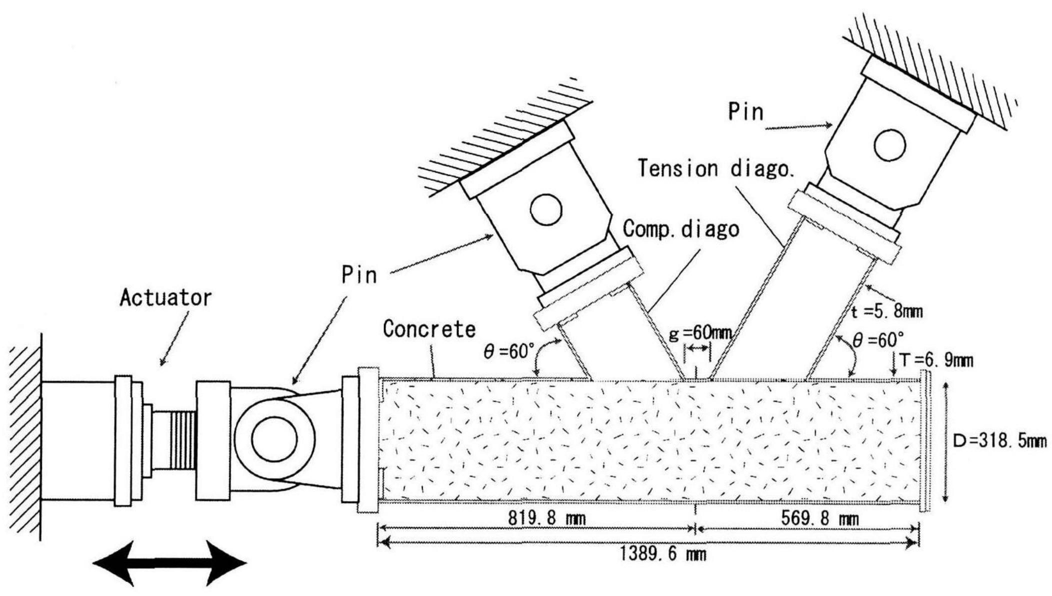

Fig.4 Test specimen configuration and support conditions

Therefore, by restraining displacement along thickness direction is not only reducing the stress concentration but also improving stability of the wall due to buckling.

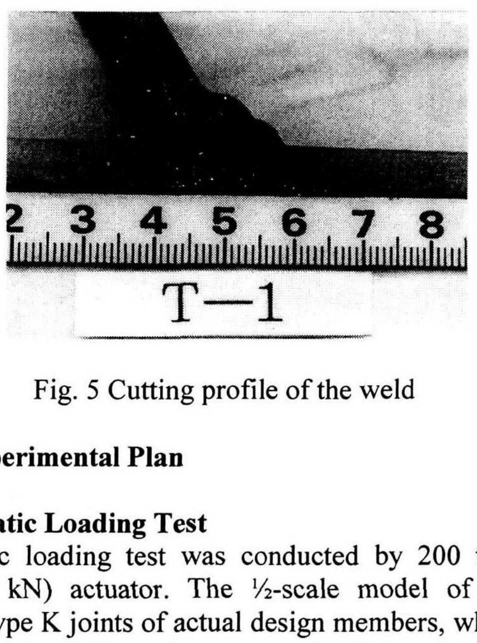

Fig. 5 Cutting profile of the weld

4. Experimental Plan

4.1 Static Loading Test

Static loading test was conducted by 200 tons (1962 kN) actuator. The ½-scale model of the prototype K joints of actual design members, which are type I and II specimens named KU-1 and KU-2. Fabrication of the test specimens was made by JIS STK 400 steel class. Yield and ultimate strengths of the chord and the diagonal members are 379 MPa, 432 MPa and 369 MPa, 459 MPa, respectively. For filled concrete, 13 cm. in concrete slump and 5% entrained air are obtained just after mixing process. Average ultimate strength of 30.1 MPa is obtained at 14 days age. Both specimens were tested under an increasing load regime whereby the maximum applied load was increased by 10 tons for first 3 cycles of loading and unloading sequences. Then, the load was incrementally applied until failure occurs. This load regime could give an effective checking of strain gage conditions within linear behavior portion of the specimens.

4.2 Fatigue Test

The fatigue tests comprised four specimens. The ½-scale model that are two hollow section (type I) K joints and two concrete filled (type II) joints were mounted to 50 tons (490 kN) actuator and pin support rigs as shown in Fig.4. The K joint fatigue tests were conducted under constant amplitude loading. These loads are 16 tons (from 1-17tons,9.8-166.7 kN) and 19 tons (from 1-20 tons,9.8-196 kN) with frequency of 3 Hz. Determination of the load ranges could be obtained through the fatigue designed curve which induce enough high stress concentration for making fatigue crack along with predicted fatigue life. The strain gauges of stress concentration type and rosette type were applied to the specimens at the position of expected hot spot stress. These locations had been confirmed by FEM prior to the experimental program.

Table 1 Fatigue test specimens

Specimen	Type	Applied load (tons)
KF-1	I	1-20 (196 kN)
KF-2	II	1-20 (196 kN)
KF-3	I	1-17 (166.7 kN)
KF-4	II	1-17 (166.7 kN)

Table 2 Summaries of static loading test specimens

Specimen	Type	Yield strength (kN)	Ultimate strength (kN)	Right end displacment at ultimate (mm)	Failure mode
KU-1	I	300	682	27	Chord buckle
KU-2	II	500	1221	23	Diagonal buckle

Fabrication of the test specimens were made by the same JIS STK 400 steel class and the material testing was carried out under axial testing of samples from the chord and the diagonal members. Yield and ultimate strengths of the chord and the diagonal members are 379 MPa, 432 MPa and 369 MPa, 459 MPa, respectively. The filled concrete has properties as 12.5 cm. slump, 4.5% entrained air and average ultimate strength of 26.3 MPa is obtained at 14 days age. The specimens KF-1, KF-2, KF-3 and KF-4 correspond to specimen types and applied loads are shown in Table 1

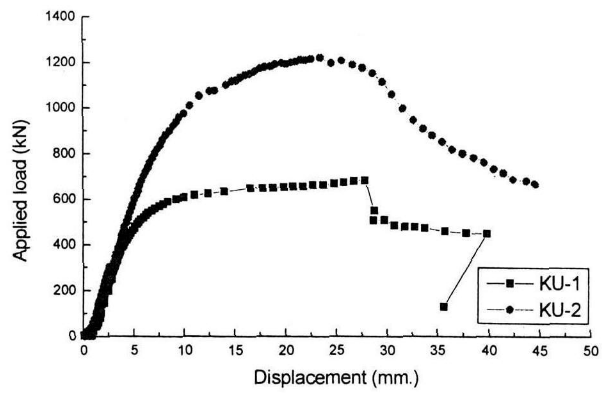

Fig.6 Testing load-displacement

5. Results of Static Loading and Fatigue Tests

5.1 Results of Static Loading Test

All the testing results, e.g. yield strengths, ultimate strengths, right end displacements and failure modes are summarized in Table 2.

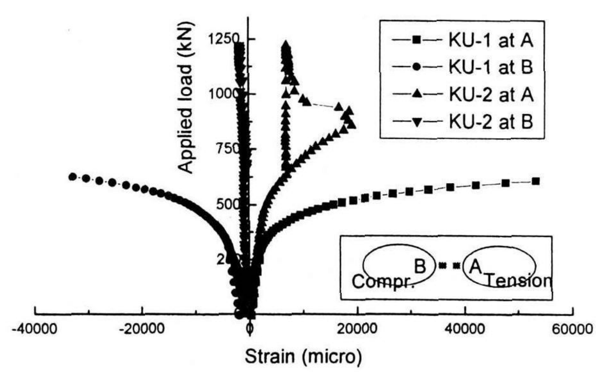

Fig.7 Local strain-applied load curves

Specimen KU-1

Fig.6 shows plots of applied load and displacement at chord right end. The specimen KU-1 gives smaller value of ultimate load about 682 kN. Under 0-200 kN, the specimen behaved elastically. After that the curve tends to be plastic with yielding of the chord near to the weld toe of compression diagonal and tension diagonal at 300 kN and 400 kN, respectively. Around 400 kN, the small crack initiated at welded toe of inner crown nearby the tension diagonal. The crack became bigger and bigger and there was not much increase in the load until it failed. Finally, failure mode was

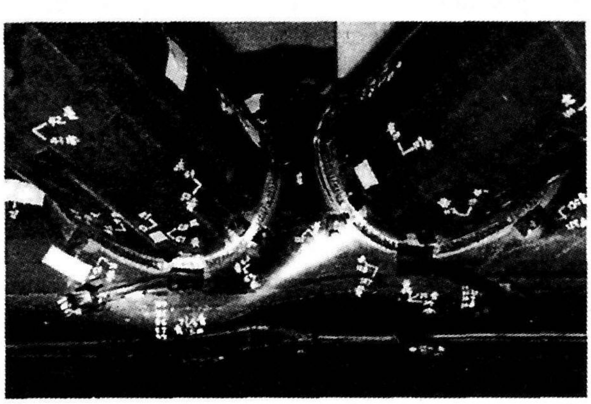

Fig.8 Failure mode of hollow specimen (KU-1)

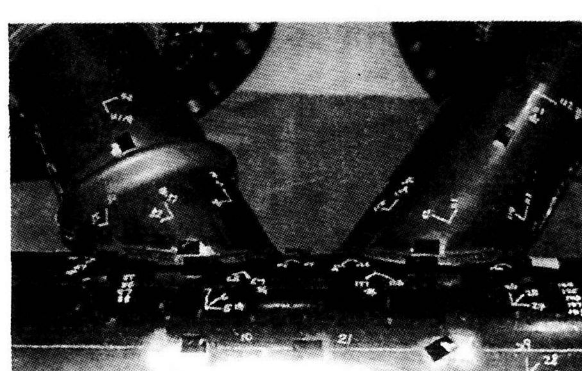

Fig.9 Failure mode of filled concrete specimen (KU-2)

observed as chord buckle and tearing of the weld (see Fig.8).

Specimen KU-2

The filled concrete section behaved elastically until 500 kN where tension diagonal became plastic. When the load was increased up to 1000 kN, displacement was rapidly increased. Until reaching 1200 kN, local buckling of diagonal wall was observed at inner side. The buckling surface became bigger by increasing small amount of applied load. Whole cross-section of the compression diagonal was totally buckled and lost its stability at 1221 kN (see Fig.9). This ultimate strength is about two times higher than the first specimen (KU-1).

Local strain at distance 4 mm. from weld toe near to tension diagonal (point A) and compression diagonal (point B) were plotted in Fig.7. The strains of the filled concrete specimen are substantially decreased compare to the hollow specimen. So the stress is much suppressed and avoids buckling of the chord wall.

From the plots (Fig.6), stiffness of specimen KU-2 and specimen KU-1 are almost the same during linear portion. However, when the specimen KU-1 yielded, it rapidly plastic hardened because of large deformation of the chord wall. The specimen KU-2 can go further with restraining concrete inside the chord. That is the deformation of the chord wall will be less and enhance some more applied load until the diagonal member reaching failure. The specimen KU-2 can show a significant increase of ultimate strength and yield a very good post-buckling behavior as from its sectional behavior of the diagonal member. In contrast, the specimen KU-1 failed suddenly.

5.2 Results of Fatigue Test

Stress distribution around the joint is much concentrated at the gap location. By checking the rosette gauges, the maximum principal stress direction could approximately represent by the stress along the direction of applied load. In order to shake out the residual stress, the stress distributions were obtained at 20 tons (196 kN) load of the third cycles loading. The stress distributions along the gap of chord wall in between the compression and tension diagonals obtained from the test of both KF-1 and KF-2 specimens are shown in Fig.10. Plot origin is at half distance between the diagonals. The strain gauges of concentration type were put at distance 4 mm. from the weld toe. Since, at closed point to weld toe, the stress distributions are very sensitive due to a very

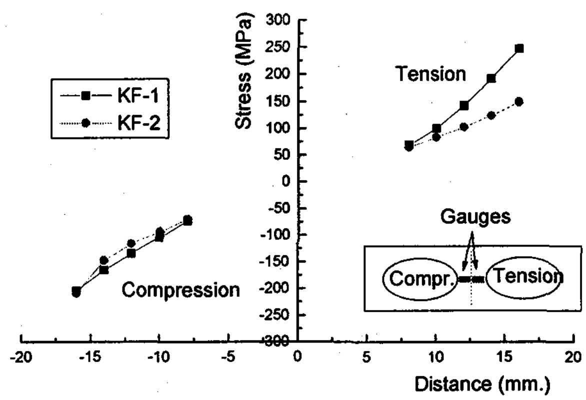

Fig.10 Stress distribution along the gap

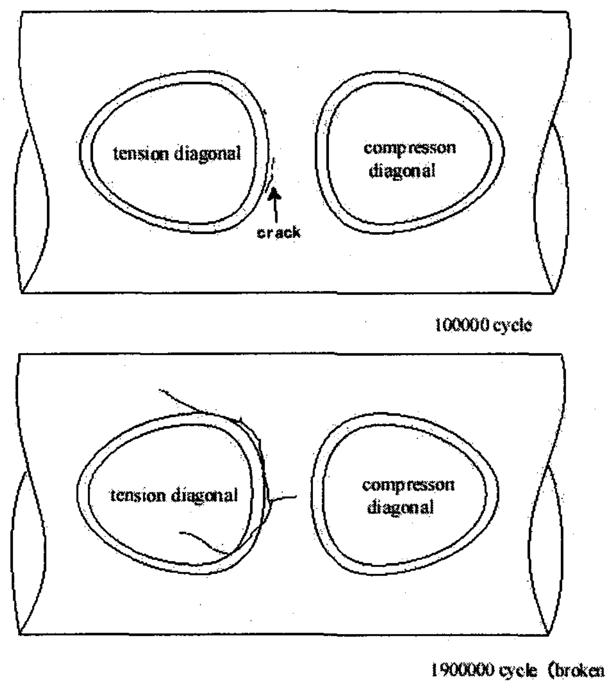

Fig.11 Cracks in specimen KF-3

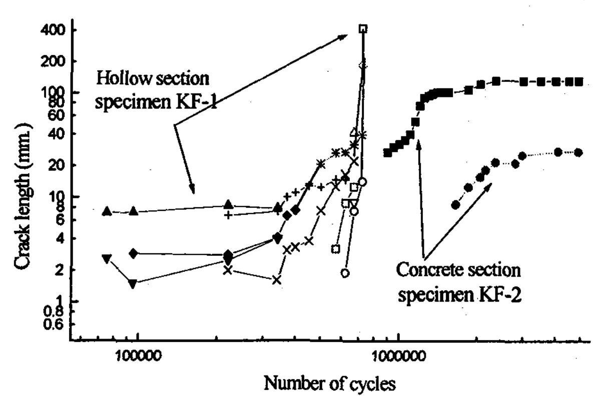

Fig.12 Crack propagation

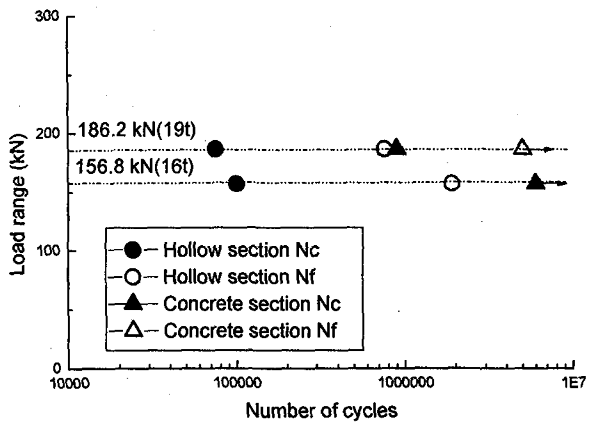

Fig.13 Fatigue life

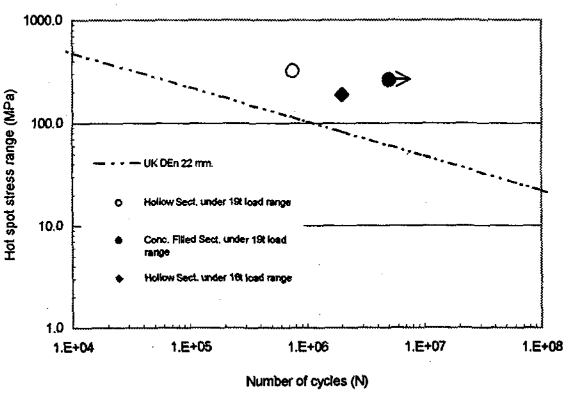

Fig.14 Fatigue strengths

high bending deformation, notch zone area, weld size, weld profile and specimen fabrication. Even a few millimeter mispositioning may cause significant changes of the obtained stresses. So, special care must be made.

Next, we found that there is about 30% reduction of the stress concentration closed to weld bead of tension diagonal. But, at close to compression diagonal, the stress distributions do not much reduce. Therefore, investigation of the filled concrete condition might tell us the interface behaviors as well as force transferring mechanism. That will be done in the next study.

Fig.11 shows the cracks that appeared in the specimen KF-3. Under the constant amplitude loading, a deep through crack was developed and propagated from the crown chord side near to tension diagonal as expected. In the filled section, up to 700000 cycles, we could not detect any crack on the surface of the chord. Until 950000 cycles, 29.8 mm. crack was suddenly found near to compression diagonal of the chord side and the crack began to propagate. Plots of crack length and number of cycles are shown in Fig.12. The filled section shows an improvement of fatigue strength, especially, the cracks seem to be stable at higher number of cycles. For the hollow specimen KF-1, crack propagation rate is faster until reaching failure condition. Influence of filled concrete to the fatigue strength is to restrain local deformation of the wall. So stress intensity will not much increase at the crack tip during the fatigue crack propagation.

Fig.13 shows plots of applied load range against number of cycles. Crack initiation point at 5 mm. and detected crack point at failure were denoted as Nc and Nf, respectively. Comparison of both specimen types indicates fatigue life improvement of the filled concrete specimen.

Later, fatigue strengths were expressed in terms of hot spot stress and number of cycles. The hot spot stresses were defined as extrapolated stresses at weld toe location from measured stress distributions (see section 6.2). In Fig. 14, the hot spot stress and fatigue life Nf of the specimens were plotted along with UKDEn (United Kingdom Department of Energy)[2] 22 mm designed curve. The hot spot stress range of the concrete filled section under the same load condition decrease as results increasing in the number of cycles. The filled concrete section gives higher fatigue strength than the hollow section. All obtained result plots show higher fatigue strength than the designed curve.

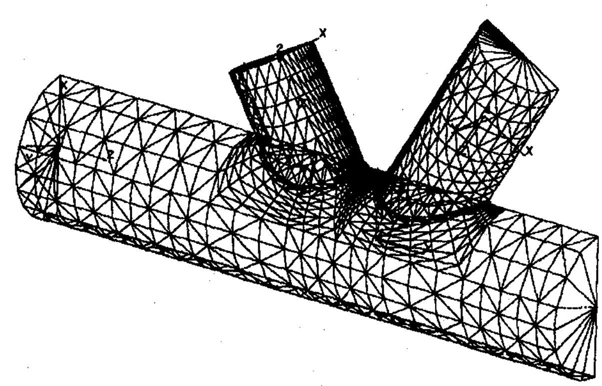

Fig.15 Finite element mesh

6. Analytical study

6.1 FEM Model

Three-dimensional nonlinear finite-element models were developed to investigate behavior of the joints. ABAQUS analysis code[3] was used for all nonlinear analytical modeling. The steel tube was model using triangular 3-node thick shell element and the concrete filled was modeled using tetrahedral 4-node solid element. Inelastic material and geometric nonlinear behavior were used for these elements. The steel behavior was assumed to be bilinear elastic-plastic model based on von Mises yield criteria defining the yield surface. The concrete was assumed to be linear elastic. Finite element mesh sensitivity test was also carried out to compare with a very refined mesh model resulting an optimized 6000 elements model as shown in Fig.15.

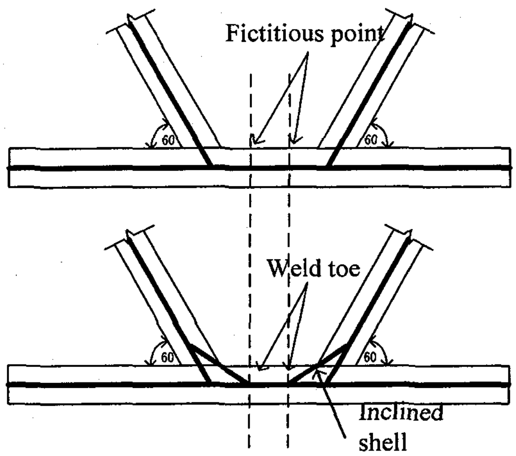

Fig.16 Weld and no weld models

The interface between the steel and the concrete was modeled using gap element. Faces of the interface were defined as free surface of the solid elements and the inner side of the shell elements. When the faces were in contact, normal force developed between two materials, therefore, frictional force will be mobilized. On the contrary, if the gap element was in tension, the contact surface separated from each other resulting in no bond developed. The bonds between the interface were modeled into 4 categories in order to correlate with experimental results; e.g. frictionless model, friction model and firmly bonded model. A coefficient of friction of 0.25 (Schneider et.al.[4]) and 0.5 were used for the friction models. The frictional force is linearly proportional to the applied normal force multiplied by the friction coefficient. When the shear force between the interface is greater than the frictional force, sliding displacement is occurred. The firmly bonded model was firmly bonded between both of the faces with no normal separation and sliding displacements. The weld profile around the diagonal-chord intersection was modeled by using an inclined shell with the thickness equals to the chord. And, no weld profile models also were made in order to compare to stress distribution to the weld models as shown in Fig.16.

Results of all analytical models were reported based on 20 tons applied force. By checking, stress-applied load relations from 0-20 tons at closed to the location of peak stress, the relations are still in linear proportion to each other. So, SCFs could represent well through the applied load with in linear region. Table.3 shows finite element model labels, type of joints, existing of weld profile and friction condition of the contact surfaces.

Table 3 Finite element models

Model	Type	Weld	Friction coef.
MK-1	I	No	--
MKW-1	I	Yes	--
MK-2A	II	No	--
MK-2B	II	No	0.25
MK-2D	II	No	Firmly bonded
MKW-2A	II	Yes	--
MKW-2B	II	Yes	0.25
MKW-2C	II	Yes	0.50
MKW-2D	II	Yes	Firmly bonded

6.2 Stress Concentration Determination

The governing parameter for an S-N approach to fatigue is the hot spot strain range or the hot spot stress range perpendicular to the weld bead. The extrapolation methods are the combination of linear and parabolic curves obtained by curve fitting through all the points in and around the region of extrapolation considered based on ECSC (European Coal and Steel Community) recommendation[5]. These methods were applied to both experimental results and the FEMs. When geometrical hot spot stress is intended to use as reference stress, weld profile and size effects must be addressed as recommended by Marshall et al.[6]. The SCFs of the experimental results and the welded FEM were determined at the weld toe location. But, for the no welded FEM, the SCFs were determined at fictitious point at the distance of weld leg length.

Parametric equations of SCFs of hollow tubular joints from various researchers, Efthymiou et al.[7], Wordsworth et al.[8], Morgan and Lee et al.[9] and etc. were used to compare with SCFs obtained from the finite element analyses and the experiments as shown in Table 4.

Table 4 SCFs from parametric equations

Parametric Equations	SCF
Ethymiou[7]	6.89
Wordsworth[8]	5.52
Morgan/Lee[9]	6.32
Kaung[10]	7.38
UK Guidance[2]	5.52

6.3 Analytical Results

It appears that maximum stress concentration occurs at the inner crown location of chord side for the hollow section model (Type I). However, in the

Table 5 SCFs from experimental results and finite element analyses

Test results		SCF	
		Combined liner and parabolic curve	
	Specimen	Tension diagonal	Compression diagonal
Including weld profile	KF-1	6.81	5.38
	KF-2	4.16	5.51
	KF-3	4.70	4.72

Finite Element Model		SCF	
		Combined liner and parabolic method	
	Model	Tension diagonal	Compression diagonal
Not including weld profile	MK-1	4.49	4.60
	MK-2A	2.78	1.98
	MK-2B	2.79	1.97
	MK-2D	0.20	0.21
Including weld profile	MKW-1	6.19	6.58
	MKW-2A	4.05	3.09
	MKW-2B	4.06	3.09
	MKW-2D	0.88	1.22

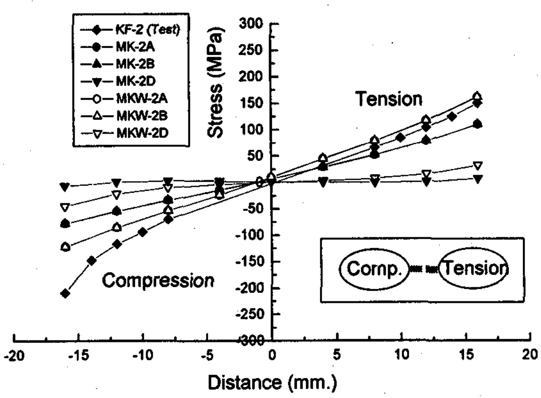

Fig.17 Stress distribution of weld and no weld models

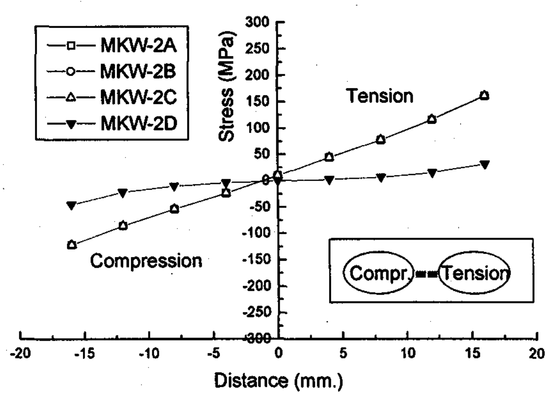

Fig.18 Stress distribution of type II models

concrete filled sections (Type II), the maximum stress concentration locations are influenced by the filled concrete especially contact condition between both surfaces. The maximum stresses of the frictionless model and the friction models occurred at the inner crown location of chord side and debonding between the two surfaces giving highest separation was observed about 20-40 degrees from the inner crown point closed to the intersection of the tension diagonal and the chord. In contrast, for firmly bonded models (MK-2D and MKW-2D) the maximum stress is at the diagonal member side near to the inner crown. That might be seen from fatigue test where fatigue crack initiated as same location as expected maximum stress concentration of the analytical results. Influence of weld profiles can affect the obtained hot spot stress. So, weld and no weld profile models were plotted in Fig 17. This figure shows a plot of stress distribution at the inner crown location versus distance along the gap. As compared to the testing results (KF-2), the weld models show a better correlation than the no weld models. This was explained in terms of extrapolated hot spot stress at the actual weld toe location.

As shown in Fig.18, when we compare 4 FEMs (MKW-2A, MKW-2B, MKW-2C and MKW-2D) together, the firmly bonded model (MKW-2D) gives the lowest of the value of stress distribution on the chord side. In addition, there are the same values of the stress distribution between the friction models (MKW-2B, MKW-2C) and the frictionless model (MKW-2A). These imply, the friction coefficient does not play an important role to the stress distribution. Hence, the separation causes no frictional force transferred as mentioned in the above section. The stress distributions depend greatly on the bending deformation of the chord wall. Therefore, in order to reduce stress effectively, sufficient restrained member must be provided as leading to further study of partial steel stiffener at under chord crown position. The model MKW-2D does not simulate debonding effect well, as vertical tension forces could be transferred to the concrete, very small stress distributions were obtained when compared with those testing results.

6.4 Comparison of analytical and testing results

Table 5 shows the SCFs obtained from the FEMs and the testing results at the crown of chord side. The magnitude of stress concentration reduced when compared with those unfilled joints. The parametric equations give the SCF in between 5.52-7.38 range. The SCFs obtained from the FEMs and the test results of the 20tons-hollow section with including weld profiles are comparatively in the order of acceptable one. Disregarding of weld profile, the obtained SCFs are rather small at the fictitious location. Furthermore, there is about 30-40% reduction of SCF at near to the tension diagonal of concrete filled joint (type II) compared to unfilled joint (type I).

7. Conclusions

Both of concrete filled and hollow K joint sections were studied. The main results of the study may be summarized as follows:

1. Concrete filled section reduces stress concentration at the intersection position. At the same load range, higher fatigue life is obtained.
2. Finite element analysis can effectively simulate composite mechanism as well as comparative results with the experimental results.
3. Friction coefficient does not play an important role to the stress distribution along the gap between both diagonals.
4. Concrete filled sections show an improvement of fatigue strength as well as ultimate strength.

Acknowledgments

The authors gratefully acknowledge Dr. Akira ISOE, Kawasaki Heavy Industry for his help on static loading test.

References

1) Morohan, D. J., New Data on Fatigue and Ultimate Limit State of Grouted Tubular Joints, Offshore Technology Conference, Houston, 1996.
2) Department of Energy, Offshore Installations: Guidance on Design and Construction, 1984.
3) ABAQUS User's Manual, Version 5.8, Habbit, Karlsson and Sorenson Inc., Providence, RI, 1998.
4) Schneider, S.P., Axially Loaded Concrete-Filled Steel Tubes, Journal of Structural Engineering, ASCE, pp. 1225-1138, 1998.
5) Puthli, R.S., Foeken, R.J. van, and Romeijn, A., Guidelines on the Determination of Stress Concentration Factors of Circular and Rectangular Hollow Section Joints, Fatigue in Offshore Structures Book, Edited by W.D. Dover, and A.G. Madhava Rao, Balkema Publishers, 1996.
6) Marshall, P.W., Design of Weld Tubular Connections, Elsevier Publishers, 1992.
7) Efthymiou, M., Development of SCF Formula and Generalized Influence Functions for use in Fatigue Analysis, Proceedings of Offshore Tubular Joints Conference, Univ. of Surrey, 1988.
8) Wordsworth, A.C., Stress Concentration Factors at K and KT Tubular Joints, Fatigue in Offshore Structural Steels, Proc. of a Conf. organized by the Institute of Civil Engineers, London, U.K., pp. 59-66, 1981.
9) Morgan, M.R. and Lee, M.M.K., New Parametric Equations for Stress Concentration Factors in Tubular K-Joints under Balanced Axial Loading, Int. J. Fatigue Vol. 19, No. 4, pp. 309-317, 1997.
10) Kuang, J.G., Stress Concentration in Tubular Joints, Paper OTC 2205, Offshore Technology Conference, Texas, 1977.

(Accepted 17/Sep/1999)